Modeling a residential microgrid for energy management

1st Martín A. Alarcón
UTN - Regional Reconquista, Santa Fe, Argentina
martinalarcon11@gmail.com

2nd Rodrigo G. Alarcón
UTN - Regional Reconquista, Santa fe, Argentina
rodrigoalarcon11@gmail.com

3rd Alejandro H. González
INTEC, CONICET - UNL, Santa Fe, Argentina
alejgon@santafe-conicet.gov.ar

4th Antonio Ferramosca
CONICET, UTN - Regional Reconquista, Santa Fe, Argentina
ferramosca@santafe-conicet.gov.ar

***Abstract*—This article proposes a discrete time model for the energy management of a residential microgrid. It consists on array of solar panels, a storage system (made up of a lithium-ion battery bank) and a load profile in line to the one of a typical residence. It is considered that it can operate connected to the main electrical network. The way to determine the loads is indicated, as well as the way to obtain the power profile generated through simulation models and the modeling of batteries that make up the storage system. The goal of the work is to obtain a suitable model to implement Model Predictive Control (MPC) strategies in the management of microgrid energy resource.**

***Index Terms*—Microgrid, Renewable Energy, Energy Management, Distributed Generation**

I. Introduction

Electric power generation is mainly based on the consumption of fossil fuels. The continuous increase in demand, the inevitable depletion of these fuels and the need for sustainable and environmentally friendly sources of generation led in recent years to the development and application of renewable generation sources.

Including, efficiently and safely, renewable energies, with their intermittent and random characteristics at their generation level, in a hierarchical, unidirectional and centralized structure, such as the current and traditional electrical system, is a challenge for the scientific community. Thinking of an electrical network, made up of smaller managements and control units, where energy storage systems are incorporated, emerges as a structural solution to handle this type of problem. In such a context, the concept of microgrid is born, proposed by [1]. A microgrid can be defined as a set of loads, energy generation and storage systems, which is seen as a single controllable system for the main electrical network, being able to operate in isolation or connected and interacting with the network. This idea is in line with the concept of distributed generation, which considers, in its simplest formulation, sources of generation on a small scale and close to the points of consumption, thus reducing energy losses produced in transmission and distribution.

A microgrid can have different scales, such as supplying energy to hospitals, university campuses, industrial parks or a domestic residences. These microgrids are the previous step for the conception of more complex systems, such as *smart grids*, where conventional and renewable generation, consumers and energy storage of different nature and size are integrated in an efficient, sustainable and safe way. This idea of the electrical network in a radial, bidirectional and decentralized way, where consumers lose their status of passive agents, and can act as one more active agent in the electricity market, is the evolution of the current energy system.

This article proposes a linear state space model of a residential microgrid for its energy management, which is composed by a renewable generation source (photovoltaic panels), a storage system (consisting of a lithium-ion battery bank), and an energy demand according to a domestic residence needs.

The note is organized as follows: in Section II the general microgrid formulation, its architecture and the different elements that compose it are described. Then, in section III, proposes the linear state space model of the microgrid is proposed. Finally, in Section IV, some conclusions are drawn.

II. Modeling

The architecture of the proposed microgrid model is shown in Figure 1, where the different elements and the energy exchange flows between them can be observed. In both, the electrical network and the battery bank, this flow is bidirectional, consisting of purchase or sale of energy, for the first, and charge or discharge for the battery, for the second. In the proposed model, these flows represent the *manipulated variables*.

To obtain a specific model, the different components are sized, starting by defining an energy consumption for a typical residence, by obtaining a daily load profile, and then, based on this, selecting the arrangement of photo-voltaic panels and the generated power. These variables, by virtue of their typical characteristics of intermittence and randomness, due to consumers behavior and climatic conditions, are considered as *non-manipulated variables or disturbance*. Also from this established consumption, the battery bank is characterized to later obtain a dynamical model of it.

It is worth noting that the hybrid inverter, in addition to making the necessary conversions for the correct operation of

ISBN: 9789874685926

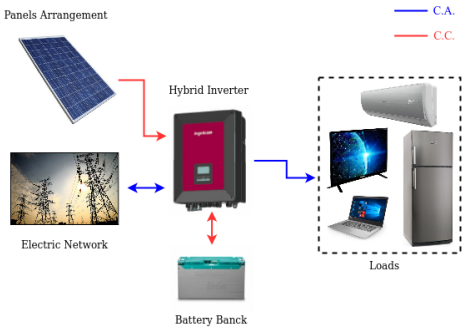

Figure 1. Residential microgrid

the system, is the node or DC bus of the microgrid. Thus, *Kirchhoff's current law* must be fulfilled.

A. General model

The general model of a microgrid can be represented by the following linear time-invariant discrete time system:

$$x(k+1) = Ax(k) + Bu(k) + Cd(k) \quad (1)$$

$$E_u u(k) + E_d d(k) = 0 \quad (2)$$

where the state variables $x(k) \in \mathbb{R}^n$ represent the load states for the storage systems in the microgrid, $u(k) \in \mathbb{R}^m$ are the manipulated variables, $d(k) \in \mathbb{R}^l$ are the disturbances or non-manipulated variables, while $A \in \mathbb{R}^{n\times n}$, $B \in \mathbb{R}^{m\times n}$, $C \in \mathbb{R}^{l\times n}$, $E_u \in \mathbb{R}^{m\times 1}$ y $E_d \in \mathbb{R}^{l\times 1}$ are matrices with the corresponding dimensions.

Equation (1) describes in a general form the dynamics of the system; while equation (2), corresponds to Kirchhoff's current law at the microgrid node. The latter can also be considered as the *energy balance* in the DC Bus, when dealing with manipulated and non-manipulated variables, with respect to the powers of the constituent elements of the system.

B. Load profile

For the determination of daily load profile, the total load of the domestic residence is first determined, as established in [2], considering an average degree of electrification. Once this is obtained, the different loads of equipment or household appliances of a residence are assigned and an usage time is estimated for each of them.

In the Table I, there is a list of the most common equipment in a house, specifying its unit power and the estimated hours of operation in a day.

For the elaboration of daily demand profile, the loads of these equipment are distributed during the day, in the most frequent hours of use. According to the indications shown Table I, the profile of Figure 2 is obtained.

C. Power generated

The renewable generation source available in the microgrid is solar energy. This is undoubtedly the most abundant and easily accessible source, which, together with wind power, are

Table I
EQUIPMENT POWER AND UTILIZATION

Equips	Quantity	Power (kW)	Use (h)
Lamp LED 9 W	6	0,009	6
TV LED 32-50"	2	0,11	2
Notebook	1	0,022	4
Refrigerator with freezer	1	0,1	24
Electric water heater	1	1,5	0,25
Air conditioning (2200 fg)	1	1,41	4
Washing machine	1	0.37	1
Microwave, kettle and iron	1	3,15	0,32
Various	1	0,65	0,16

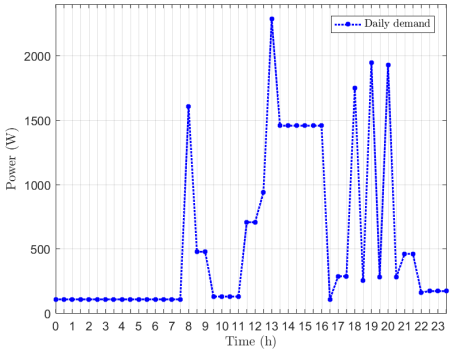

Figure 2. Load profile

among the most developed clean energy sources. Its choice as renewable source in the model of a residential microgrid is based on the relative simplicity of application, installation and maintenance required to obtain electrical energy through photovoltaic panels.

The characteristics of the chosen panels are detailed in Table II.

Table II
POLY-CRYSTALLINE PANEL TSM-330PD14 TECHNICAL SPECIFICATIONS

Dates	Description
Nominal power, P_{max}	330 W
Voltage at maximum power point, V_{mpp}	$37,4$ V
Maximum current, I_{mpp}	$8,83$ A
Open circuit voltage, V_{oc}	$45,8$ V
Short circuit current, I_{sc}	$9,28$ A
Module efficiency, η_m	$0,17$

The number of panels that conform the arrangement is obtained by taking the daily consumption of the house, what is indicated in Table I, making a total of $12,98$ kWh. By considering the indicated power of the panel and assuming four peak sun hours $(HSP = 4)$, the following number is obtained:

$$N^o_{panels} = \frac{Q_{diary} \cdot 1,2}{HSP \cdot P_{max}} = \frac{12,98\,(kWh) \cdot 1,2}{4\,(h) \cdot 0,33\,(kW)} \approx 12 \quad (3)$$

These panels can be connected in different ways, in series, parallel or mixed. In this work, the connection will be mixed, 2 groups of 6 panels in series and these, in turn, connected in parallel, thus obtaining the electrical characteristics indicated in Table III. This choice depends on the characteristics of the used inverter.

Table III
HONEYCOMB ARRAY ELECTRICAL PARAMETERS

Dates	Description
Nominal power, P_{max}	3960 W
Voltage at maximum power point, V_{mpp}	224, 2 V
Maximum current, I_{mpp}	17, 66 A

The power generated by this installation of a photovoltaic source is obtained by using the mathematical model of a cell and therefore of the panel, since this is a set of series-parallel connected cells, attached on a metal plate encapsulated by a thermal insulator. As dynamical model, the one proposed by [3], which consists of obtaining the electrical output characteristics, using an equivalent electrical circuit, depending on the solar irradiance and cell temperature as it is shown Figure 3.

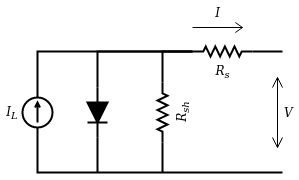

Figure 3. Equivalent circuit solar cell [3]

These electrical output characteristics show non-linear current-voltage and power-voltage relationships.

This mathematical model is implemented in a block called **"PV Array"** in Matlab-Simulink, where the user can load the characteristics of preset panels or define one with specific parameters. The nonlinear behavior of the panel presented in Table II , with the solar irradiance and reference cell temperature values, is shown in Figure 4.

Given the low efficiency of photovoltaic panels, it is necessary to use control strategies to operate them at their maximum power point (MPPT) all the time, independently of variations in irradiance and temperature. Furthermore, given that voltage level generated in the panels is generally not sufficient, therefore, it will be necessary to elevate it to appropriate levels, efficiently as possible. This is achieved through the implementation of a structure made up of a DC converter and an MPPT control algorithm, which allows the monitoring of the maximum power point [4]. This system is implemented in the hybrid inverter indicated in Figure 1. The converter selected is of the type **Boost** [5] and the MPPT algorithm is of the kind disturb and observe **P&O** [6], which tracks the maximum power point, modifying the converter's duty cycle.

In order to obtain a profile of the power generated in one day (similar to what was done for the consumption of a house,

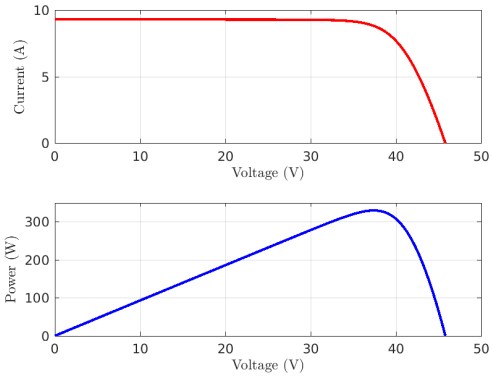

Figure 4. Characteristic curves of the poly-crystalline panel TSM-330PD14 para $G_{ref} = 1000\ (W/m^2)$ y $T_{c,ref} = 25^oC$.

since both are considered as not manipulated variables in our model) the Matlab-Simulink scheme indicated in the Figure 5 is taken into account, where the considered panel arrangement is modeled by using the block **"PV Array"** and the DC converter and the MPPT algorithm are implemented, to obtain the desired power profile.

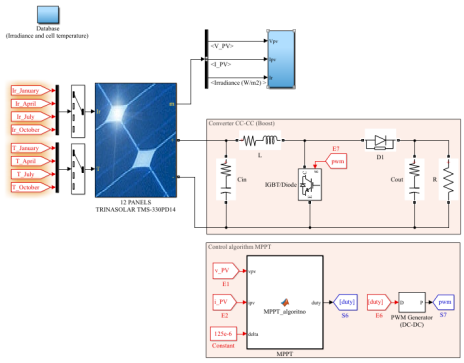

Figure 5. Scheme for obtaining the generated power profile

As it can be seen, the scheme made for the simulation is able to load various irradiance and temperature curves, in order to obtain different power profiles generated in different months of the year and different climatic conditions.

The irradiance and cell temperature data are obtained from [7]. If the data is considered for a sunny January day, for the city of Avellaneda, Santa Fe - Argentina, the power generated by the panel arrangement is indicated in the Figure 6.

D. Battery bank

The energy storage system is made up of a lithium-ion battery bank, the characteristics of which are specified in the Table IV.

To determine the number of batteries that will make up the bank, daily consumption of the residence is selected as $Q_{diary} = 12,98$ kWh, while the inverter efficiency is given by $\eta_{inv} = 0,955$ and the admissible voltage for the bank connection, imposed by the characteristics of the inverter, in this case is $V_{b,bat} = 48$ V.

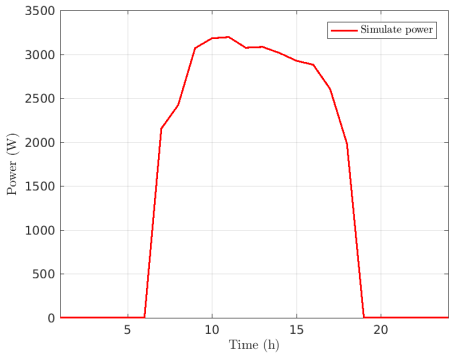

Figure 6. Generated power profile

Table IV
BATTERY-MLI ULTRA 12/5500 TECHNICAL SPECIFICATIONS

Dates	Description
Nominal voltage, V_{bat}	12 V
Nominal capacity, C_{bat}	400 Ah
Useful life (cycles), N_c	3500
Efficiency, η_{bat}	$0,90$

As the microgrid will have access to the electrical network and with the goal of reducing the number of batteries in the bank, since these are the most expensive components, it is considered a 50% of daily consumption, 2 days of autonomy $d_a = 2$ and bank discharge depth (DOD) $Pf_{des} = 0,8$ to guarantee the 3500 life cycles. Therefore, the bank's capacity is given by:

$$C_{b,bat} = \frac{0,5 \cdot Q_{diary} \cdot d_a}{V_{b,bat} \cdot \eta_{bat} \cdot Pf_{desc} \cdot \eta_{inv}} = 393,27(\text{Ah}) \quad (4)$$

while the number of batteries is obtained from:

$$N_{bat} = \frac{V_{b,bat} \cdot C_{b,bat}}{V_{bat} \cdot C_{bat}} = 3,93 \quad (5)$$

As a result, 4 batteries are adopted which will be connected in series. The characteristics of the batteries bank are detailed in Table V.

Table V
BATTERY BANK TECHNICAL SPECIFICATIONS

Dates	Description
Number of batteries, N_{bat}	4
Nominal capacity, $C_{b,bat}$	400 Ah
Nominal voltage, $V_{b,bat}$	48 V
Connection type	serie

To determine the dynamic behavior of the battery and therefore of the bank, a model based on an equivalent electrical circuit proposed by [8] is considered, which can be seen in Figure 7.

It consists of two separate circuits, which are related to each other by a voltage controlled voltage source and a current

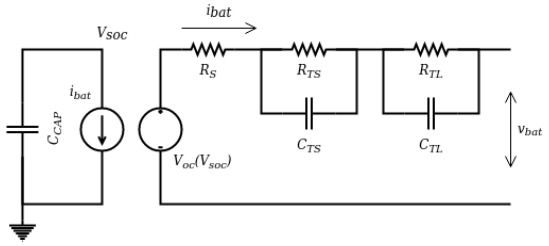

Figure 7. Equivalent battery circuit [8]

controlled current source. The one on the left models the storage capacity and the stored load during the loading or unloading processes. The one on the right describes internal resistance and transient behavior for different loads.

To determine the values of the components of circuit, the method of extraction of parameters in the time domain proposed by [9] is applied, which is based on analyzing the characteristics of the voltage curve in the relaxation period of the battery, after applying a discharge or charge pulse.

The test is carried out by mounting a simulation platform in Matlab-Simulink, using as the battery to test, the block **Battery** available in the software (see Figure 8).

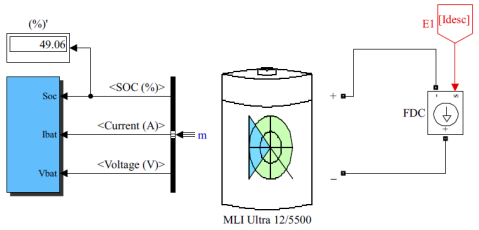

Figure 8. Test to obtain parameters

The chosen methodology will be to apply a constant discharge current pulse for a certain time, followed by a relaxation period where the voltage in the battery is allowed to autonomously stabilize, and then reapply the current pulse. The adopted values for the current and times are: $i_{pulse} = 173$ A, $t_{pulse} = 420$ s y $t_{rela.} = 30$ min.

The resistance and capacities of the equivalent circuit vary according to the state of charge of battery. (SOC, and therefore it depends on the V_{soc}, open circuit voltage), therefore, different values will be obtained for different load states for which the test is performed.

Resistance R_s is first determined as:

$$R_S = \frac{V_{t_v} - V_{t_v^+}}{i_{pulse}} \quad (6)$$

where V_{t_v} is the open circuit voltage and $V_{t_v^+}$ is the voltage 1 second after the discharge current is applied. Figure 9 shows the time evolution of the voltage and current when the discharge pulse is applied.

Then the relaxation period is divided into temporary windows. It will have as many windows as RC branches has the circuit. In this case they go from $t_{11} = 471$ s to $t_{12} = 473$ s

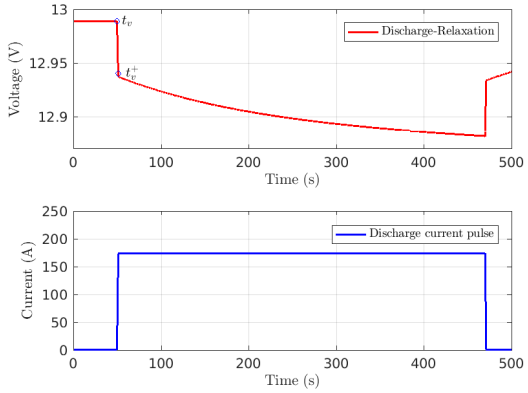

Figure 9. Voltage in the battery when applying the discharge pulse

and $t_{21} = 1500$ s to $t_{22} = 1800$ s. When taking into account these times, it should be considered that t_{21} must be at least 3 times greater than t_{12}, and t_{22} must be prior to the moment when voltage at the battery terminals reaches the stable state. See Figure 10.

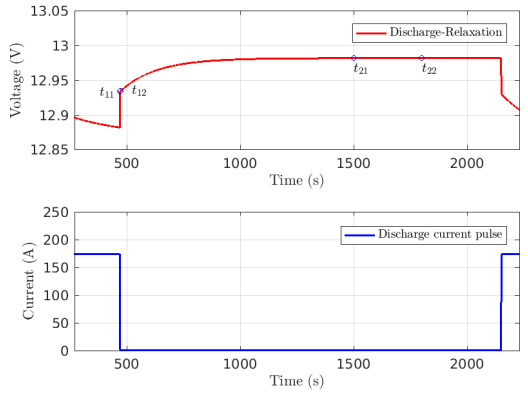

Figure 10. Battery voltage in the relaxation period

To get R_{TL} y C_{TL}, the instantaneous voltage drops are first calculated at t_{21} y t_{22}:

$$V_{t_{21}} = V_{oc} - V_{bat_{21}} \tag{7}$$

$$V_{t_{22}} = V_{oc} - V_{bat_{22}} \tag{8}$$

Where $V_{bat_{21}}$ y $V_{bat_{22}}$ are obtained from the test. Therefore, the time constant τ_{TL} is given by:

$$\tau_{TL} = \frac{t_{22} - t_{21}}{\ln\left(\frac{V_{t_{21}}}{V_{t_{22}}}\right)} \tag{9}$$

The initial voltage is determined in t_{21}, $U_{TL} = V_{t_{21}} \cdot e^{\frac{t_{21}}{\tau_{TL}}}$; and with this R_{TL} y C_{TL}:

$$R_{TL} = \frac{U_{TL}}{i_{pulse} \cdot \left(1 - e^{-\frac{t_{pulse}}{\tau_{TL}}}\right)} \tag{10}$$

$$C_{TL} = \frac{\tau_{TL}}{R_{TL}} \tag{11}$$

Now, is calculated R_{TS} y C_{TS}. To do that, the instantaneous voltage drops in t_{11} and t_{12} are obtained:

$$V_{t_{11}} = V_{oc} - V_{bat_{11}} - V_{TL}(t_{11}) \tag{12}$$

$$V_{t_{12}} = V_{oc} - V_{bat_{12}} - V_{TL}(t_{12}) \tag{13}$$

where $V_{TL}(t) = U_{TL} \cdot e^{-\frac{t}{\tau_{TL}}}$.

The time constant τ_{TS} will be:

$$\tau_{TS} = \frac{t_{12} - t_{11}}{\ln\left(\frac{V_{t_{11}}}{V_{t_{12}}}\right)} \tag{14}$$

As in the previous case, the initial tension in t_{11} is $U_{TS} = V_{t_{11}} \cdot e^{\frac{t_{11}}{\tau_{TS}}}$, so that:

$$R_{TS} = \frac{U_{TS}}{i_{pulse} \cdot \left(1 - e^{-\frac{t_{pulse}}{\tau_{TS}}}\right)} \tag{15}$$

$$C_{TS} = \frac{\tau_{TS}}{R_{TS}} \tag{16}$$

Different values of R_S, R_{TL}, C_{TL}, R_{TS} and C_{TS} are obtained according to the initial SOC. Then, to validate the model, to analyze its behavior and to be able to choose the values with which smallest maximum relative error occurs in different scenarios, the equivalent circuit is built in Matlab-Simulink.

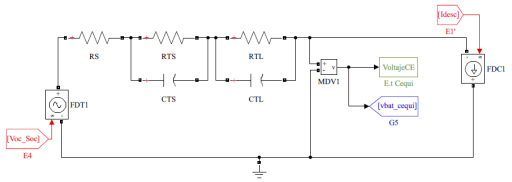

Figure 11. Equivalent circuit in Matlab-Simulink

In order to simulate the voltage controlled voltage source, it will be necessary to find a function $V_{OC} = f(SOC)$ that relates the state of charge with the open circuit voltage. For this, different tests are performed to find the curve, and then using the **MATLAB-Curve Fitting Tool**, the curve is adjusted using the following function for the analyzed battery:

$$V_{OC} = -9,126 \cdot SOC^{-0,9876} + 13,11 \tag{17}$$

The values identified for a $SOC = 80\%$ are the ones that produce the least relative error in dynamic behavior under different conditions, so these will be the ones used in the model. The analyzed range goes from 20 % to 80 %, which is the band where batteries must work according to the manufacturer's recommendations, for the depth of discharge adopted.

To obtain the continuous-time state space model, it is considered that the SOC can be described by the *Coulomb Count Method*:

$$SOC = SOC_0 \pm \frac{1}{C_{cap}} \int i_{bat} dt \tag{18}$$

By Kirchhoff's Laws in the circuit of Figure 7, in the meshes of RC branches and considering as state variables $\dot{x}_1 = \frac{\partial SOC}{\partial t}$, $\dot{x}_2 = \frac{\partial V_{TS}}{\partial t}$ and $\dot{x}_3 = \frac{\partial V_{TL}}{\partial t}$, as input $u = i_{bat}$ and as output $y = v_{bat}$ it is obtained:

$$\dot{x} = \begin{bmatrix} 0 & 0 & 0 \\ 0 & -\frac{1}{R_{TS}C_{TS}} & 0 \\ 0 & 0 & -\frac{1}{R_{TL}C_{TL}} \end{bmatrix} x + \begin{bmatrix} \frac{1}{C_{bat}} \\ \frac{1}{C_{TS}} \\ \frac{1}{C_{TL}} \end{bmatrix} u \tag{19}$$

$$y = \begin{bmatrix} 1 & -1 & -1 \end{bmatrix} x + \begin{bmatrix} R_S \end{bmatrix} u \tag{20}$$

Then, by replacing the values obtained from the test for battery bank, we have:

$$\dot{x} = \begin{bmatrix} 0 & 0 & 0 \\ 0 & -6.28e^{-3} & 0 \\ 0 & 0 & -2.87e^{-5} \end{bmatrix} x + \begin{bmatrix} 9.08e^{-7} \\ 3.78e^{-6} \\ 7.03e^{-8} \end{bmatrix} u \tag{21}$$

$$y = \begin{bmatrix} 1 & -1 & -1 \end{bmatrix} x + \begin{bmatrix} 0.0002 \end{bmatrix} u \tag{22}$$

If the previous model is discretized by the method of *Tustin* with a sampling period $T_s = 3600$ s, which is the time interval which the charge and generation profiles are elaborated with, we obtain the following discrete-time model of the battery bank:

$$x(k+1) = \begin{bmatrix} 1 & 0 & 0 \\ 0 & -0.85 & 0 \\ 0 & 0 & 0.9 \end{bmatrix} x(k) + \begin{bmatrix} 3.26e^{-3} \\ 1.11e^{-3} \\ 2.41e^{-4} \end{bmatrix} u(k) \tag{23}$$

$$y(k) = \begin{bmatrix} 1 & -0.08 & -0.95 \end{bmatrix} x(k) + \begin{bmatrix} 1.16e^{-3} \end{bmatrix} u(k) \tag{24}$$

III. Dynamical Model of the Microgrid

The microgrid model will have a single state corresponding to the only storage system, the battery bank. The manipulated variables will be the bank's discharge/charge powers (Pb_d/Pb_c) and those corresponding to the purchase/sale with the electrical network (Pn_p/Pn_s). The power generated by the solar panels and the determined load profile are the non-manipulated variables (P_{gen}/P_{load}).

By explicitly considering as manipulated variables the discharge and charge powers of the battery bank (Pb_d/Pb_c), the obtained model of the bank, taking everything that enters the microgrid node with positive sign, everything that leaves the node with negative sign, and taking into accoubt the general formulation presented in Section II-A, one gets:

$$x(k+1) = x(k) + \begin{bmatrix} k_1 & k_2 & 0 & 0 \end{bmatrix} u(k) \tag{25}$$

$$\begin{bmatrix} 1 & -1 & 1 & -1 \end{bmatrix} u(k) + \begin{bmatrix} 1 & -1 \end{bmatrix} d(k) = 0 \tag{26}$$

where $x(k) = SOC$, k_1 y k_2 are constants that depend on the model of the bank, $u(k) = \begin{bmatrix} Pb_d & Pb_c & Pn_p & Pn_s \end{bmatrix}^T$ is the array of manipulated variables and $d(k) = \begin{bmatrix} P_{gen} & P_{load} \end{bmatrix}^T$ is the array of the non-manipulated variables.

To determine the values of k_1 y k_2, it should be considered that when modeling the battery bank, the manipulated variable was the current i_{bat}, which could be loading or unloading, while now it is considered the power $Pb_{d/c}$. Moreover, by taking the inverter efficiency as $\eta_{inv} = 0,955$ and its effect is the direction of discharge/charge of the bank, and by setting $V_{ref} = V_{b,bat} = 48$ V, which is the nominal voltage of the inverter for connection of th storage system, then:

$$k_1 = -\frac{100 \cdot 3.26e^{-3}}{V_{ref} \cdot \eta_{inv}} = -7.11e^{-3} \tag{27}$$

$$k_2 = \frac{100 \cdot 3.26e^{-3} \cdot \eta_{inv}}{V_{ref}} = 6.48e^{-3} \tag{28}$$

IV. Conclusions

A discrete-time linear state space model of a microgrid was presented. A way of considering and modeling the different factors involved is shown, resulting in a starting point to model more complex systems, such as microgrids with other sources of generation or storage. This model will be used to evaluate advanced control techniques for energy management in the microgrid.

References

[1] B. Lasseter, "Microgrids [distributed power generation]," in *2001 IEEE power engineering society winter meeting. Conference proceedings (Cat. No. 01CH37194)*, vol. 1. IEEE, 2001, pp. 146–149.

[2] A. Asociación Electrotécnica Argentina, "Reglamentación para la ejecución de instalaciones eléctricas en inmuebles. viviendas, oficinas y locales (unitarios)," AEA 90364-7-771. CABA, Argentina, Tech. Rep., 2016.

[3] W. Xiao, W. G. Dunford, and A. Capel, "A novel modeling method for photovoltaic cells," in *2004 IEEE 35th Annual Power Electronics Specialists Conference (IEEE Cat. No. 04CH37551)*, vol. 3. IEEE, 2004, pp. 1950–1956.

[4] H. A. Meza, J. L. M. García, and S. S. Mora, "Estrategias de control mppt aplicadas en un convertidor dc/dc tipo boost para sistemas fotovoltaicos," *REVISTA COLOMBIANA DE TECNOLOGIAS DE AVANZADA (RCTA)*, vol. 2, no. 30, 2018.

[5] L. D'Alessio, L. González, and R. Cáceres, "Diseño y construcción de un convertidor boost de pequeña potencia, con propósitoseducativos y de investigación," *ACI Avances en Ciencias e Ingenierías*, vol. 6, no. 2, 2014.

[6] L. Ruiz, J. Beristáin, I. Sosa, and J. Hernández, "Estudio del algoritmo de seguimiento de punto de máxima potencia perturbar y observar," *Revista de ingeniería eléctrica, electrónica y computación*, vol. 8, no. 1, 2010.

[7] N. R. E. Laboratory, "Pvwatts calculator," Recuperado de https://pvwatts.nrel.gov/index.php, 2019.

[8] M. Chen and G. A. Rincon-Mora, "Accurate electrical battery model capable of predicting runtime and iv performance," *IEEE transactions on energy conversion*, vol. 21, no. 2, pp. 504–511, 2006.

[9] A. Hentunen, T. Lehmuspelto, and J. Suomela, "Time-domain parameter extraction method for thévenin-equivalent circuit battery models," *ieee transactions on energy conversion*, vol. 29, no. 3, pp. 558–566, 2014.